Advantages of water droplet machining over abrasive waterjet cutting of carbon fiber reinforced polymer

Mitchell, Benjamin; Sadek, Ahmad; Kinsey, Brad

Publisher’s version / Version de l'éditeur:
https://doi.org/10.1016/j.mfglet.2022.07.041
Manufacturing Letters, 33, S, pp. 342-348, 2022-09-16

Available online at www.sciencedirect.com

Manufacturing Letters

Manufacturing Letters 33 (2022) 342–348

50th SME North American Manufacturing Research Conference (NAMRC 50, 2022)

Advantages of water droplet machining over abrasive waterjet cutting of carbon fiber reinforced polymer

Benjamin Mitchell[a], Ahmad Sadek[b], Brad Kinsey[a,*]

[a]Department of Mechanical Engineering, University of New Hampshire, 33 Academic Way, Durham, NH 03824, USA
[b]Aerospace Manufacturing Technologies Center, National Research Council, Montreal, QC, Canada

* Corresponding author. *E-mail address:* brad.kinsey@unh.edu

Abstract

The cutting of carbon fiber reinforced polymer (CFRP) sheets with conventional tooling, such as an end-mill, results in excessive tool-wear, high-heat generation, and dust emission. Abrasive waterjet (AWJ) cutting has been used as an alternative method; however, this technique often leads to delamination of the composite material, especially around the pierce locations. Moreover, AWJ requires considerable post processing of the machined part to remove residual abrasive particles in addition to the high nozzle and conduit wear rates. A new advancement in pure waterjet cutting, Water Droplet Machining (WDM), has shown success in cutting CFRP sheets without the detrimental effects of delamination. In this paper, the results of cutting 5.5mm-thick CFRP sheet are presented using an AWJ and the WDM process. The cutting performance of the two methods is assessed based on the surface roughness of the cut edge, the presence of delamination, and the geometric accuracy of a variety of basic shapes cut from the sheet.

Keywords: Carbon fiber reinforced polymer; waterjet cutting; delamination.

1. Introduction

Carbon fiber reinforced polymer (CFRP) composites are heterogeneous and anisotropic materials, which exhibit high stiffness, excellent corrosion-resistance, and high strength-to-weight ratios, and thus offer superior functional performance over conventional materials, such as steel [1]. These advantageous properties have led to widespread manufacturing and adoption of CFRP in a variety of industries including aerospace, automotive, marine, medical, sporting equipment, and wind energy [2]. During CFRP manufacturing, the composite is typically molded into the desired part geometry; however, subsequent machining operations, such as trimming, tapering, and hole drilling, are often required to bring the part into tolerance and to create features that would not be possible with the layup process alone. Creating these features with conventional tooling, such as a drill or end-mill, often result in excessive tool-wear, high-heat generation, composite delamination, and dust emission [2, 3]. Delamination and heat-induced resin degradation compromise CFRP part quality, which is particularly concerning for aircraft manufacturers as a single, large aircraft contains over a million mounting holes [2, 3, 4]. Delamination-related failures of aircraft components have led to rejection rates as high as 60% [3]. Despite these manufacturing challenges, studies have been conducted in an attempt to identify machining parameters, which mitigate delamination, increase the machinability of CFRP, and extend tool life by the use of slow feed rates and spindle speeds, specialized tool geometries and coatings, and minimized lubricant levels [5-13]. Even with these methodologies, the risk of delamination and part degradation persists, requiring consistent quality monitoring, which adds to the already high tooling and machining costs of CFRP production. Therefore, alternative manufacturing techniques are sought, which produce high-quality edge features at low production costs.

Laser beam cutting has been used for CFRP hole drilling and edge routing, however, a heat affected zone is generated which has limited its widespread use in cutting CFRPs [2, 3, 14-16]. Abrasive waterjet (AWJ) cutting has been used as another alternative CFRP cutting process, but this technique often leads to delamination of the composite material, especially around pierce locations. To mitigate delamination, through-holes can be pre-drilled in the composite to create a starting position for the AWJ; however, the drilling process is subject to pull-up and push-out delamination [17]. When piercing CFRPs with an AWJ, the mechanism responsible for delamination is the hydrodynamic stagnation pressure created by a water-wedge action [17, 18]. The water, following the path of least resistance, will separate the layers if the pressure exceeds the tensile strength of the bonding layer. Furthermore, abrasive particles can become embedded into interlaminar cracks, requiring additional operations to remove the residual particles [19]. Despite these adverse effects of piercing and cutting CFRP with AWJ, there has been success in suppressing delamination by starting the pierce with a close to zero water pressure and then slowly increasing water pressure until the pierce is complete [20]. Varying the water pressure (and therefore, water flow rate) consequently requires fine tuning and timing of the abrasive delivery system. Various AWJ piercing techniques have been developed and are still active areas of investigation [17-23]. According to the literature and industrial correspondents, a method, which cuts CFRP with satisfactory results and with low cost of production, is still lacking. It is therefore worthwhile to explore Water Droplet Machining (WDM) as an alternative CFRP cutting technique.

WDM is a novel manufacturing technique which employs a high-velocity waterjet to produce a series of water droplets, which repeatedly impact and erode a material surface, see Figure 1 [24]. The process is conducted within a vacuum chamber to suppress aerodynamic drag and atomization of the

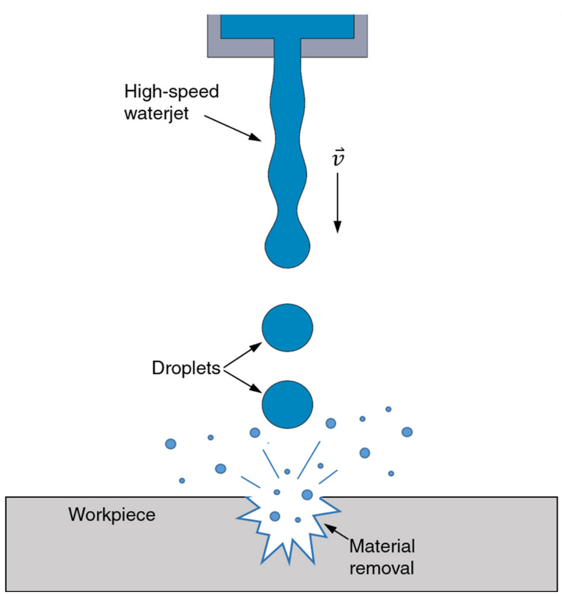

Figure 1: Diagram of the idealized Water Droplet Machining process, in through-cutting mode, using a high-speed Rayleigh jet, which produces a train of droplets that impact, erode and cut-through a workpiece.

waterjet. This preserves the waterjet momentum allowing for a more efficient transfer of energy between the water and workpiece material, than in standard atmospheric pressure. For example, the ability of WDM to cut steel with a thickness of 6.35mm has been demonstrated, although at much slower feed rates than an AWJ [25]. In the present research, a small orifice, i.e., 100μm, is used, which, with the help of the low ambient pressure, produces an axisymmetric and continuous Rayleigh jet. Downstream disturbances grow, which create a wavy jet that eventually leads to segmentation of the jet into a series of droplets. For this research, a significant distance between the orifice and workpiece, i.e., stand-off distance of 686mm, is required for effective material removal. If the stand-off distance is too small then a continuous jet impacts the workpiece, which is less effective at material removal. The WDM droplet-impact-erosion mechanism(s) are currently ill-understood; however, experiments, which measure the impact force of low-speed Rayleigh jets, show that the peak force exerted by a droplet train is about four times greater than the force induced by a continuous jet of equal momentum [26]. This suggests that a train of droplets has a higher erosive potential than a continuous jet.

Owing to the absence of abrasives and the lack of heat-affect-zone in WDM, it is worth investigating whether this manufacturing process can cut CFRPs with reasonable cut-edge characteristics and without the tendency for delamination. Therefore, the aim of this paper is to explore the CFRP cutting performance of WDM on industry relevant CFRP sheets and compare the results to similar tests conducted with an AWJ. Section 2 outlines the experimental methods used in cutting the CFRP specimens with WDM and AWJ. Section 3 discusses the results of both cutting methods and evaluates the cut characteristics based on surface roughness, the presence of delamination, and the geometric accuracy of the intended part. Section 4 highlights the main discoveries while proposing future work in WDM cutting of CFRPs.

2. Experimental Methods

To compare the effectiveness of cutting a CFRP laminate with WDM and with an AWJ, a variety of basic shapes were cut out of the CFRP workpiece. The CFRP laminate used in these tests was produced by autoclave-molding of 22 woven graphite/epoxy plies with a layup configuration of [90, $(0^{\circ}/90^{\circ})_5$]s. The autoclave pressure was 516.75 kPa and the cure time was 60 min at 127 °C. The final cured laminate thickness was 5.5± 0.02 mm. The cut out shapes were a series of circles ranging from 1mm to 32mm, an equilateral triangle of side length 30mm, and a raster path of side length 50mm. The AWJ used was a Wardjet E-1515 with a Hypertherm Hyprecision 60s intensifier pump. This is also the same water pump used in WDM experiments, which produces a water pressure of 414MPa. The abrasive cutting head uses a 406μm diameter orifice, a 1.016mm diameter nozzle, an abrasive flow rate of 476 grams/minute, an 80-mesh abrasive, and a stand-off distance of 3mm. According to the Hypertherm cutting calculator, 5.5mm-thick CFRP should be cut at a feed rate of 1600mm/min for excellent edge quality [27]. Faster feed rates can also be used to cut the CFRP but at reduced edge quality.

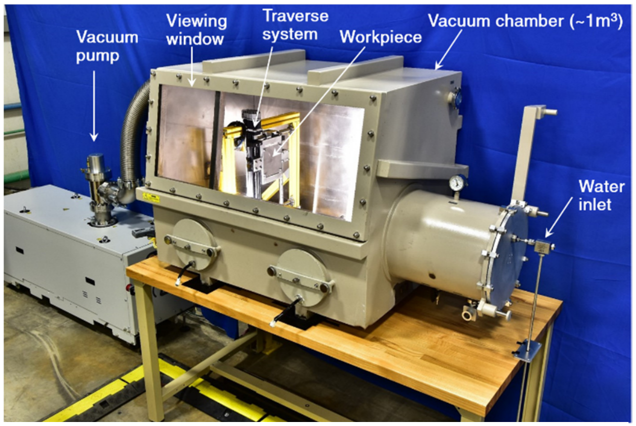

Figure 2: Image of experimental setup showing a workpiece mounted onto the traverse system inside vacuum chamber.

For these experiments a 1600mm/min feed rate was chosen so that the highest quality edge would be produced. For stationary piercing, which is the piercing method used in these experiments, the Hypertherm cutting calculator suggests using low pressure, 103MPa, for 1 second, then increasing the pressure to 414MPa to perform the remainder of the cut. The piercing procedure turns the jet on at low pressure and then 0.2 seconds later the abrasive flow starts, which was found to be the most successful timing for mitigating delamination [20]. One second later the pump switches to high pressure, which takes 3.5 seconds to achieve, and then proceeds to move along the tool path. This method was used in all AWJ pierces. To mitigate delamination around the shape edges, all pierces start in the middle of each circle and triangle. Then the jet traverses up to the shape edge and finally moves around the outline. This positions the pierces as far away from the feature edges as possible.

For the WDM experiments, which are conducted inside a $1m^3$ vacuum chamber, see Figure 2, a water pressure of 414MPa was used for all piercing and cutting procedures. An orifice diameter of 100µm was used with a stand-off distance of 686mm. The pressure and temperature inside the chamber during cutting were 5.3 torr and 3℃, respectively. Note that WDM operates close to the triple point of water, which is the temperature and pressure at which water exists in equilibrium in its liquid, solid, and gaseous states. Contrary to Figure 1, the waterjet used in the experiments is horizontal, which is done so that large stand-off distances can be accommodated. All pierces are dwelled for 1 second and then the jet moves relative to the workpiece. The feed rate used was 60mm/min, although 120mm/min was also explored as detailed in Section 3.2.

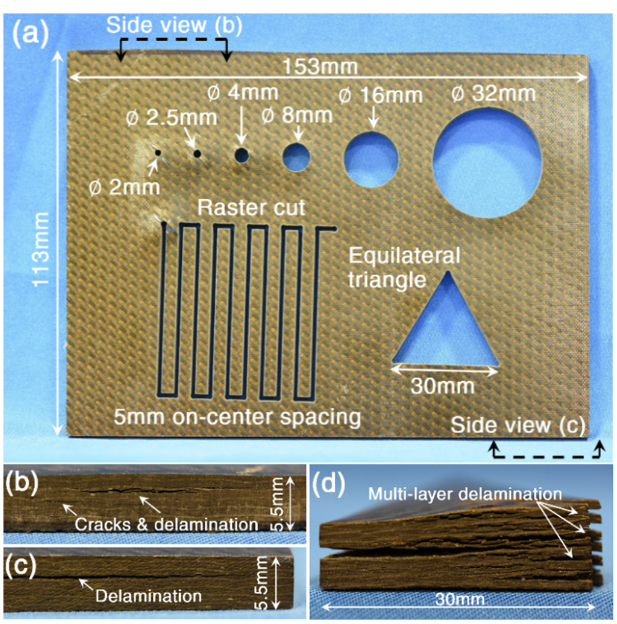

Figure 3: (a) Top view of various shapes cut in a CFRP sheet with AWJ, (b) side view of top-edge, (c) side view of bottom-edge, and (d) side view of cut out triangle showing delamination features.

3. Results and Discussion

3.1. Abrasive waterjet cutting of CFRP

Figure 3(a) shows the CFRP sample cut using AWJ. It is apparent that the process created the desired shapes but with moderate delamination in some regions. Around each circle the upper surface of the sample is raised while cracks are visible on the inside edges. The smallest hole, which is roughly 2mm in diameter, is a pierce only, i.e., the jet does not traverse the circumference. The top-edge of the sample closest to this hole shows edge delamination and cracking as shown in Figure 3(b), with the location of the side view indicated in Figure 3(a). This edge is about 30mm away from the hole location, which indicates that the delamination phenomena can spread far away from pierce locations. A similar feature exists on the bottom edge of the sample closest to the triangle, see Figure 3(c), with the location of the side view again indicated in Figure 3(a). The inside of the shapes, which contain the pierce, all show severe delamination. Figure 3(d) shows a side of the cut out triangle with significant multi-layer delamination. It is not surprising that considerable delamination occurs near pierce locations as this is where the water wedge action occurs [17]. For the raster path, the pierce starts in the upper left corner and has a 5 mm on-center spacing between the lines. The raised surface in this region indicates that delamination occurred here; however, the remainder of the raster path appears to have excellent cut characteristics. This is the only region where delamination did not occur (based on visual observation). If an AWJ starts in a through-hole or off the part, then delamination can be avoided [20]. However, even with the low-pressure pierce option used in these experiments, delamination occurred at all pierce locations.

3.2. Water droplet machining of CFRP

For the WDM experiments, a similar tool path was made to create the same shapes as in the AWJ experiments, i.e., a series of circles, a triangle, and a raster path. Figure 4(a) shows the CFRP sample cut by WDM. Visual observation of WDM cut edges show an absence of delamination for all shapes. Note that the four holes in the corners of the sample were hand drilled for fixturing the sample onto the WDM system. The other holes, ranging from 1mm to 32mm in diameter, show good cut quality. All of the pierce locations feature a small crater-like region of hollowed-out material, roughly 1mm in size. In Figure 4(a), this is apparent on the 1mm diameter hole, which

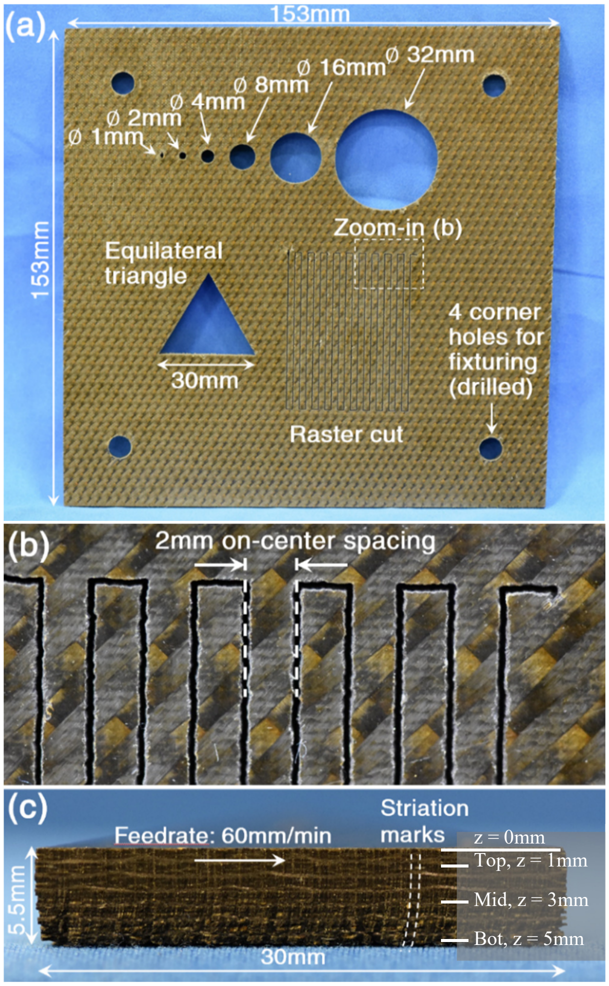

Figure 4: (a) Top view of various shapes cut in a CFRP sheet with WDM, (b) zoom-in view of raster kerf, and (c) side view of bottom-edge of triangle.

is slightly elliptical, and also on the start of the raster (top left). The cut-out circles and triangle also feature this crater effect at the pierce location (not shown in Figure 4). Figure 4(b) shows a zoomed-in image of the raster cut. These cuts are separated by 2mm on-center spacing between the lines, which would not have been possible with the AWJ since this jet's kerf width is slightly greater than 1mm. Figure 4(b) also elucidates the small kerf widths, i.e., 300µm, achievable with WDM. The consistency of this diminutive kerf is remarkable considering how far away the orifice is from the sample, i.e., stand-off distance to kerf ratio of 2287. This is achievable because of the low ambient pressure and its negligible effects on the waterjet and droplet train, i.e., so that atomization does not occur.

The circles and triangle cuts were performed with a feed rate of 60mm/min, while the raster was cut with a feed rate of 120mm/min. This feed rate was slightly too fast as the CFRP is still attached in some areas on the bottom-side of the cut. This is apparent if the sample is held up to a light and visually inspected by looking through the cuts. Figure 4(c) shows the bottom edge of the triangle cut-out. Note that delamination and cracks are not visually present. This is in contrast to the AWJ cut triangle edge in Figure 3(d), which showed significant delamination. On the left and right bottom corners of the triangle in Figure 4(c) the laminate appears to be chipped,

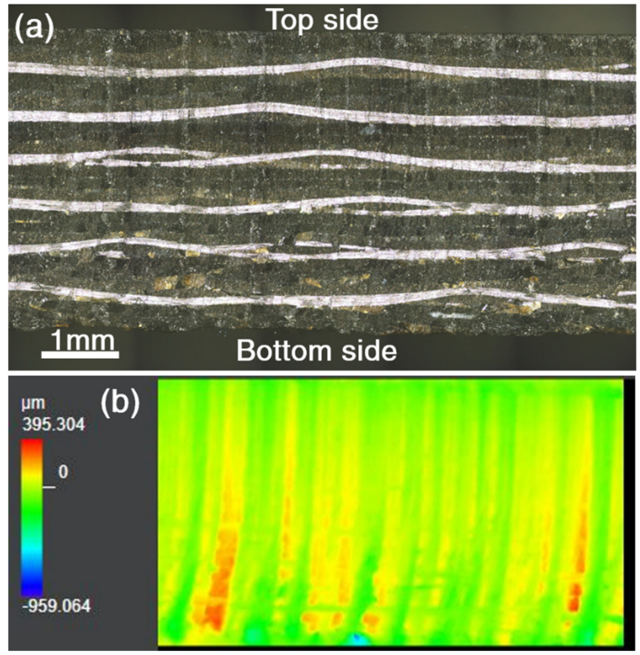

Figure 5: (a) Microscope image of WDM triangle cut edge in CFRP, and (b) topographic height-map of surface shown in (a).

where individual layers can be identified; however, these chips did not seem to propagate into the material as a delamination. Figure 4(c) also shows striation marks on the cut edge, which is a similar feature to an AWJ cut edge on metal [28].

Another unique feature of WDM is its ability to create tight corners of approximately 150µm radii. The AWJ cut triangle corners, in Figure 3(a), are notably different compared to the triangle corners cut by WDM in Figure 4(a). This feature of WDM allows for fabrication of small feature sizes in CFRP and with less risk of delamination than with AWJ. Although WDM can produce tiny kerfs and does not feature delamination, it is considerably slower at cutting CFRP than the AWJ, which is approximately 27 times faster. However, note that the AWJ technology has been heavily studied and optimized, while WDM is in its infant stages of development and so has the potential for growth and enhancement. One question that remains is the tendency of WDM to suppress delamination. Due to the discrete nature of WDM, see Figure 1, it is possible that the lateral stagnation pressure that the material experiences is periodic and at a high enough frequency so that delamination is suppressed, although more research is required to validate this notion.

3.3. Surface roughness of WDM cut edge on CFRP

Surface roughness measurements were conducted on the WDM cut-out triangle of Figure 4(c), using an Olympus OLS5000 3D laser microscope. Figure 5(a) shows a detailed microscope image of the WDM cut surface, where individual fiber layers can be identified. From this image, delamination and cracks are absent suggesting that the WDM process does not induce delamination of CFRP. Owing to the cold operating temperatures of WDM it is surmised that WDM does not cause heat-induced resin degradation either. Figure 5(b) shows a 5.5 x 9.5mm^2 topographic height map of the cut surface, revealing ridges of raised composite material, as shown by the red-

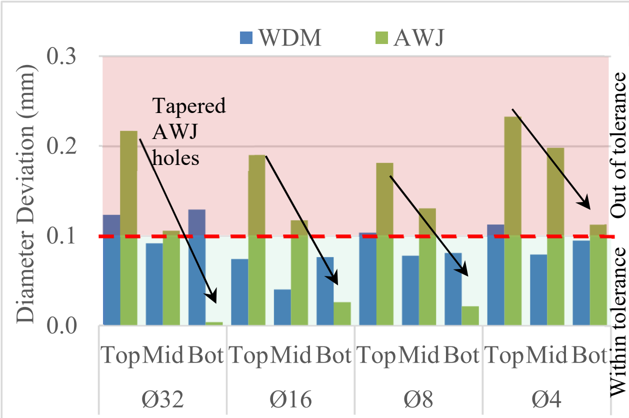

Figure 6: Hole diameter deviation measured at top, middle, and bottom level planes for the WDM and AWJ process.

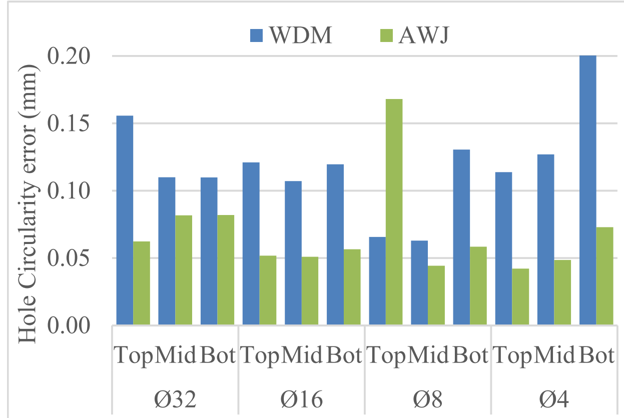

Figure 7: Hole circularity errors measured at top, middle, and bottom level planes for the WDM and AWJ process.

colored features. Note that in Figure 5(b), green is taken as the mean surface height of 0µm. The raised surface features, which are analogous to the striation marks observed in AWJ cutting of metals, have heights of approximately 300 to 400µm. The ridges increase in height from the top-side of the CFRP specimen towards the bottom-side where they are at a maximum. These ridges increase the roughness of the cut edge, and for the surface shown in Figure 5(b), the mean surface area roughness is S_a = 56.1µm. While individual fiber layers are easily identified in Figure 5(a), the same cannot be said for Figure 5(b), as the morphology of the WDM cut surface does not expose layers and is nearly homogeneous in the through-thickness direction. Due to the presence of cracks and delamination in the AWJ-cut specimen, edge roughness measurements were not performed.

3.4. Dimensional accuracy of AWJ and WDM cuts

The characterization of the dimensional and geometric accuracy of the holes and the equilateral triangle features was performed on a Mitutoyo MACH-806 coordinate measurement machine (CMM). The hole diameter and circularity errors of the Ø 32 mm, Ø16 mm, Ø8 mm and Ø4 mm holes were measured using a 2 mm diameter probe. For each hole, measurements were performed at the Top, middle (Mid) and bottom (Bot) planes located at ‘z’ depths of 1 mm, 3 mm, and 5 mm, respectively, from the uppermost plane (z = 0 mm) of the CFRP plate, as shown in Figure 4(c). Ten measurement points were probed to measure the diameter and circularity of each circular hole feature at each of such planes. Measurements of the Ø2.5 mm, Ø2 mm, and Ø1 mm holes were not possible due to the limitation of the probe size. Figure 6 compares the measured mean hole diameter deviation from the nominal hole diameter at the top, middle and bottom planes using the WDM and AWJ processes. The figure shows that both processes produced oversized hole diameters that ranged between (+0.07 mm to +0.12 mm) for the WDM and (+0.02 mm to +0.23 mm) for the AWJ. In a case where a static maximum tolerance limit of +0.10 mm was considered, the acceptance rate (within tolerance) for the WDM holes (75%) was significantly higher than that for the AWJ (25%). This could be attributed to the excessive material removal in AWJ caused by the abrasive particles in the cutting zone. The figure also shows, for all the AWJ holes, a gradual reduction of the hole size from the top to the bottom planes indicating a tapered hole surface of an average 0.86° angle. The WDM holes did not experience such effect and were found to be more cylindrical. Reducing the taper angle in AWJ may require a higher jet pressure and a reduced standoff distance to increase the cutting efficiency near the bottom [29]. Taper reduction may also be possible by changing the feed rate.

On the other hand, Figure 7 shows around two-fold higher circularity errors for the WDM compared to the AWJ machined holes at the top, middle and bottom planes. Circularity error is the radial distance between the minimum circumscribing circle and the maximum inscribing circle of the measured surface points. The lower circularity error in the AWJ-cut holes could be due to the ability of the jet and abrasive particles to facilitate sharper and smoother edges compared to the WDM jet. Alternatively, since the x-y stages for the WDM and AWJ processes are different, this could affect circularity of the features created.

The average straightness and perpendicularity errors of the equilateral triangle wall surfaces (along the depth of the plate) were computed based on three measurements per surface. The perpendicularity of the triangle wall surfaces was measured with respect to the CMM probed uppermost plane of the CFRP plate (z = 0 in Figure 4(c)). The average straightness errors of the three triangle surfaces along the depth of the plate was found to be 0.052 mm and 0.021 mm for the WDM and the AWJ processes, respectively. This agrees with the higher circularity errors observed in the case of circular holes cut via WDM compared to AWJ. In terms of the average perpendicularity errors of the triangle wall surfaces with respect to the uppermost CFRP plate surface reference, the WDM showed a relatively lower error (0.078 mm) compared to that of the AWJ (0.110 mm), which agrees with the tapered hole findings. Table 1 summarizes the test conditions and dimensional measurement results of cutting various diameter holes in CFRP with both waterjet machines. WDM showed a smaller average diameter deviation (Avg. dia. dev.) and smaller taper angle than AWJ; however, WDM had a higher average circularity error (Avg. circ. error) than AWJ.

Table 1: Test conditions and results of hole cutting.

Tool	Orifice (μm)	Feed rate (mm/min)	Avg. dia. dev. (mm)	Avg. taper (°)	Avg. circ. error (mm)
AWJ	406	1600	0.13	0.86	0.07
WDM	100	60	0.09	0.07	0.12

4. Conclusion

Experiments were used to evaluate the cutting characteristics of CFRP using two disparate waterjet cutting processes, AWJ and WDM. The AWJ created cracks and delamination regions in the CFRP despite using the low-pressure pierce capabilities of the process. The WDM successfully cut the CFRP without delamination and with fairly acceptable geometric and dimensional accuracy, although at a much slower feed rate than the AWJ. In addition, the WDM process was able to cut very narrow kerfs, indicating that small CFRP part sizes can be fabricated with WDM. The features cut from WDM showed less taper although higher circularity and straightness error than those from AWJ. Therefore, WDM demonstrated some geometrical advantages but also some disadvantages compared to AWJ. Nevertheless, this unique cutting process can be a practical solution to cutting CFRP without the tendency of delamination, heat-generation, and dust emission. Although due to the slow feed rate required in WDM, one must consider total cutting time and cost, among other aspects, to justify its use over conventional cutting techniques such as end-mill and AWJ cutting. Future studies will also investigate the CFRP cutting thickness limitation of WDM.

The favorable cutting performance of the WDM process can be seen as an achievement for pure waterjet cutting technology; however, the material removal mechanisms and the ability for WDM to cut CFRP without delamination requires further investigation. It can be reasoned that the differences in jet morphology, e.g., continuous as in AWJ, versus discrete as in WDM, lead to disparate erosion processes, which result in the presence (or absence) of delamination. Finite element analyses and micro-mechanical modeling of the droplet-composite interaction are potential avenues through which the WDM erosion mechanisms can be identified.

Acknowledgements

Support from the University of New Hampshire Graduate School and the US National Science Foundation, through award No. CMMI-1462993, is gratefully acknowledged.

References

[1] Chung D. Carbon fiber composites. Elsevier; 2012.
[2] Che D, Saxena I, Han P, Guo P, Ehmann KF. Machining of carbon fiber reinforced plastics/polymers: a literature review. Journal of Manufacturing Science and Engineering. 2014;136(3).
[3] Karataş MA, Gökkaya H. A review on machinability of carbon fiber reinforced polymer (CFRP) and glass fiber reinforced polymer (GFRP) composite materials. Defence Technology. 2018;14(4):318-26.
[4] El-Sonbaty I, Khashaba UA, Machaly T. Factors affecting the machinability of GFR/epoxy composites. Composite structures. 2004;63(3-4):329-38.
[5] Durão LM, Gonçalves DJ, Tavares JM, de Albuquerque VH, Vieira AA, Marques AT. Drilling tool geometry evaluation for reinforced composite laminates. Composite structures. 2010;92(7):1545-50.
[6] Davim JP, Reis P. Study of delamination in drilling carbon fiber reinforced plastics (CFRP) using design experiments. Composite structures. 2003;59(4):481-7.
[7] Gaitonde V, Karnik SR, Rubio JC, Correia AE, Abrao AM, Davim JP. Analysis of parametric influence on delamination in high-speed drilling of carbon fiber reinforced plastic composites. Journal of materials processing technology. 2008;203(1-3):431-8.
[8] Shahrajabian H, Hadi M, Farahnakian M. Experimental investigation of machining parameters on machinability of carbon fiber/epoxy composites. International Journal of Engineering and Innovative Technology. 2012;3(3):30-6.
[9] Shahrajabian H, Hadi M, Farahnakian M. Experimental investigation of machining parameters on machinability of carbon fiber/epoxy composites. International Journal of Engineering and Innovative Technology. 2012;3(3):30-6.
[10] Krishnaraj V, Prabukarthi A, Ramanathan A, Elanghovan N, Kumar MS, Zitoune R, Davim JP. Optimization of machining parameters at high speed drilling of carbon fiber reinforced plastic (CFRP) laminates. Composites Part B: Engineering. 2012;43(4):1791-9.
[11] Slamani M, Chatelain JF, Hamedanianpour H. Influence of machining parameters on surface quality during high speed edge trimming of carbon fiber reinforced polymers. International Journal of Material Forming. 2019;12(3):331-53.
[12] Rawat S, Attia H. Wear mechanisms and tool life management of WC–Co drills during dry high speed drilling of woven carbon fibre composites. Wear. 2009;267(5-8):1022-30.
[13] Senthilkumar M, Prabukarthi A, Krishnaraj V. Machining of CFRP/Ti6Al4V stacks under minimal quantity lubricating condition. Journal of Mechanical Science and Technology. 2018;32(8):3787-96.
[14] Pagano N, Ascari A, Liverani E, Donati L, Campana G, Fortunato A. Laser interaction with carbon fibre reinforced polymers. Procedia Cirp. 2015;33:423-7.
[15] Takahashi K, Tsukamoto M, Masuno S, Sato Y, Yoshida H, Tsubakimoto K, Fujita H, Miyanaga N, Fujita M, Ogata H. Influence of laser scanning conditions on CFRP processing with a pulsed fiber laser. Journal of materials processing technology. 2015;222:110-21.
[16] Patel P, Sheth S, Patel T. Experimental analysis and ANN modelling of HAZ in laser cutting of glass fibre reinforced plastic composites. Procedia Technology. 2016;23:406-13.
[17] John KM, Kumaran ST. Backup support technique towards damage-free drilling of composite materials: A review. International Journal of Lightweight Materials and Manufacture. 2020;3(4):357-64.
[18] Shanmugam DK, Nguyen T, Wang J. A study of delamination on graphite/epoxy composites in abrasive waterjet machining. Composites Part A: Applied Science and Manufacturing. 2008;39(6):923-9.
[19] Schwartzentruber J, Papini M, Spelt JK. Characterizing and modelling delamination of carbon-fiber epoxy laminates during abrasive waterjet cutting. Composites Part A: Applied Science and Manufacturing. 2018;112:299-314.
[20] Kim G, Denos BR, Sterkenburg R. Influence of different piercing methods of abrasive waterjet on delamination of fiber reinforced composite laminate. Composite Structures. 2020;240:112065.
[21] Schwartzentruber J, Spelt JK, Papini M. Modelling of delamination due to hydraulic shock when piercing anisotropic carbon-fiber laminates using an abrasive waterjet. International Journal of Machine Tools and Manufacture. 2018;132:81-95.
[22] Nyaboro JN, Ahmed MA, El-Hofy H, El-Hofy M. Fluid-structure interaction modeling of the abrasive waterjet drilling of carbon fiber reinforced polymers. Journal of Manufacturing Processes. 2020;58:551-62.
[23] Thongkaew K, Wang J, Li W. An investigation of the hole machining processes on woven carbon-fiber reinforced polymers (CFRPs) using abrasive waterjets. Machining Science and Technology. 2019;23(1):19-38.
[24] Mitchell BR, Demian SA, Korkolis YP, Kinsey BL. Experimental comparison of material removal rates in abrasive waterjet cutting and a novel droplet stream technique. Procedia Manufacturing. 2020;48:586-92.

[25] Guglielmi G, Mitchell B, Song C, Kinsey BL, Mo W. Life Cycle Environmental and Economic Comparison of Water Droplet Machining and Traditional Abrasive Waterjet Cutting. Sustainability. 2021 (21):12275.

[26] Mitchell BR, Klewicki JC, Korkolis YP, Kinsey BL. Normal impact force of Rayleigh jets. Physical Review Fluids. 2019;4(11):113603.

[27] https://waterjet-calculator.hypertherm.com/

[28] Orbanic H, Junkar M. Analysis of striation formation mechanism in abrasive water jet cutting. Wear. 2008;265(5-6):821-30.

[29] El-Hofy M., Helmy M.O, Escobar-Palafox G., Kerrigan K., Scaife R., El-Hofy H. Abrasive Water Jet Machining of Multidirectional CFRP Laminates. Procedia CIRP. 2018; 68: 535-540.